

Molecular architecture of copper(I) thiometalates. Synthesis and characterization of $(\text{NPr}_4)_3[\text{WS}_4\text{Cu}_5\text{I}_6]$, a cubane with two additional faces

Francis Sécheresse^{1*}, Sylvain Bernès², Francis Robert², Yves Jeannin²

¹ Laboratoire d'électrochimie et chimie de solides inorganiques, LECSI, EP CNRS J 0067,
Université de Versailles, 78035 Versailles;

² Laboratoire de chimie des métaux de transition, URA-CNRS 419,
Université Pierre-et-Marie-Curie, 4, place Jussieu, 75252 Paris Cedex 05, France

(received 9 May 1995, accepted 27 July 1995)

Summary – Reaction of $(\text{NPr}_4)_3[\text{WS}_4\text{Cu}_3\text{I}_4]$ **1**, which is prepared by addition of CuI to $(\text{NPr}_4)_2[\text{WS}_4]$, with CuCl in dichloromethane gave crystals of $(\text{NPr}_4)_3[\text{WS}_4\text{Cu}_5\text{I}_6]$ **3** (orthorhombic, space group *Pbnm* (standard *Pnma* No 62), $a = 13.130(6)$, $b = 20.829(12)$, $c = 22.715(5)$ Å, $Z = 4$, $R = 0.0504$). The crystal structure revealed discrete $[\text{WS}_4\text{Cu}_5\text{I}_6]_3^-$ anions separated by NPr_4^{4+} cations; the anionic framework consists of a $(\text{WS}_3\text{Cu}_3\text{I})$ cube with two additional faces. Addition of NEt_4Cl to $(\text{NPr}_4)_3[\text{WS}_4\text{Cu}_3\text{Br}_4]$ **2** in dichloromethane yielded red crystals of $(\text{NEt}_4)_4[\text{WS}_4\text{Cu}_5\text{Br}_7]$ **7** (monoclinic, space group *C2/c*, $a = 22.866(5)$, $b = 10.760(2)$, $c = 21.960(9)$ Å, $Z = 4$, $R = 0.0626$). The two isostructural compounds $(\text{NEt}_4)_3[\text{WS}_4\text{Cu}_5\text{Cl}_7]$ **8** and $(\text{NEt}_4)_3[\text{WS}_4\text{Cu}_5\text{Cl}_{1.5}\text{I}_{5.5}]$ **6** were characterized. The reactivity of these compounds was examined together with the relationships that exist with various copper thiometalate compounds characterized previously.

copper thiometalate / cubane structure / dicubane structure

Introduction

The tetrathiometalates MS_4^{2-} ($\text{M} = \text{Mo}, \text{W}$) have been used as versatile ligands to prepare a wide variety of heteropolynuclear complexes [1-11]. Among the various compounds structurally characterized, those containing Cu(I) were recently examined according to their Cu/ MS_4 content and their structural type [12]. These MS_4Cu_n architectures result from the step-by-step addition of CuX ($\text{X} = \text{Cl}, \text{Br}, \text{I}$) to the edges of the parent MS_4 tetrahedron as represented in figure 1. The resulting compounds are highly stabilized by the interaction of a empty *d* orbital of the central metal M (Mo(VI) , W(VI)) with a filled *d* orbital of copper (I) [13]. Another feature is the activation of the central $\text{MS}_4(\text{Cu})_n$ core by further addition of copper which led to the preparation of a large set of copper-rich polynuclear complexes including $(\text{NMe}_4)_5[\text{MoS}_4(\text{CuCl})_6\text{Cl}_2]$, the ultimate product of the addition of CuCl units across all six edges of the parent MS_4 tetrahedron [14]. To complete these studies, we describe here the preparation and characterization of new architectures together with their connections to the established structural types presented in figure 1. We also confirm the reactivity of the closed cubane structure $[\text{MS}_4\text{Cu}_3\text{X}_4]^{2-}$ ($\text{X} = \text{Cl}, \text{Br}, \text{I}$) examined in previous work [12].

Experimental section

All manipulations were carried out in a nitrogen atmosphere. Reagent grade chemicals were used throughout. Commercial CuCl was washed with a solution of HCl to eliminate Cu(II) ions. Infrared spectra were recorded on a 580B Perkin Elmer spectrophotometer (KBr pellets). Elemental analyses were performed by the Service Central d'Analyses du CNRS, Solaize, France.

Preparations

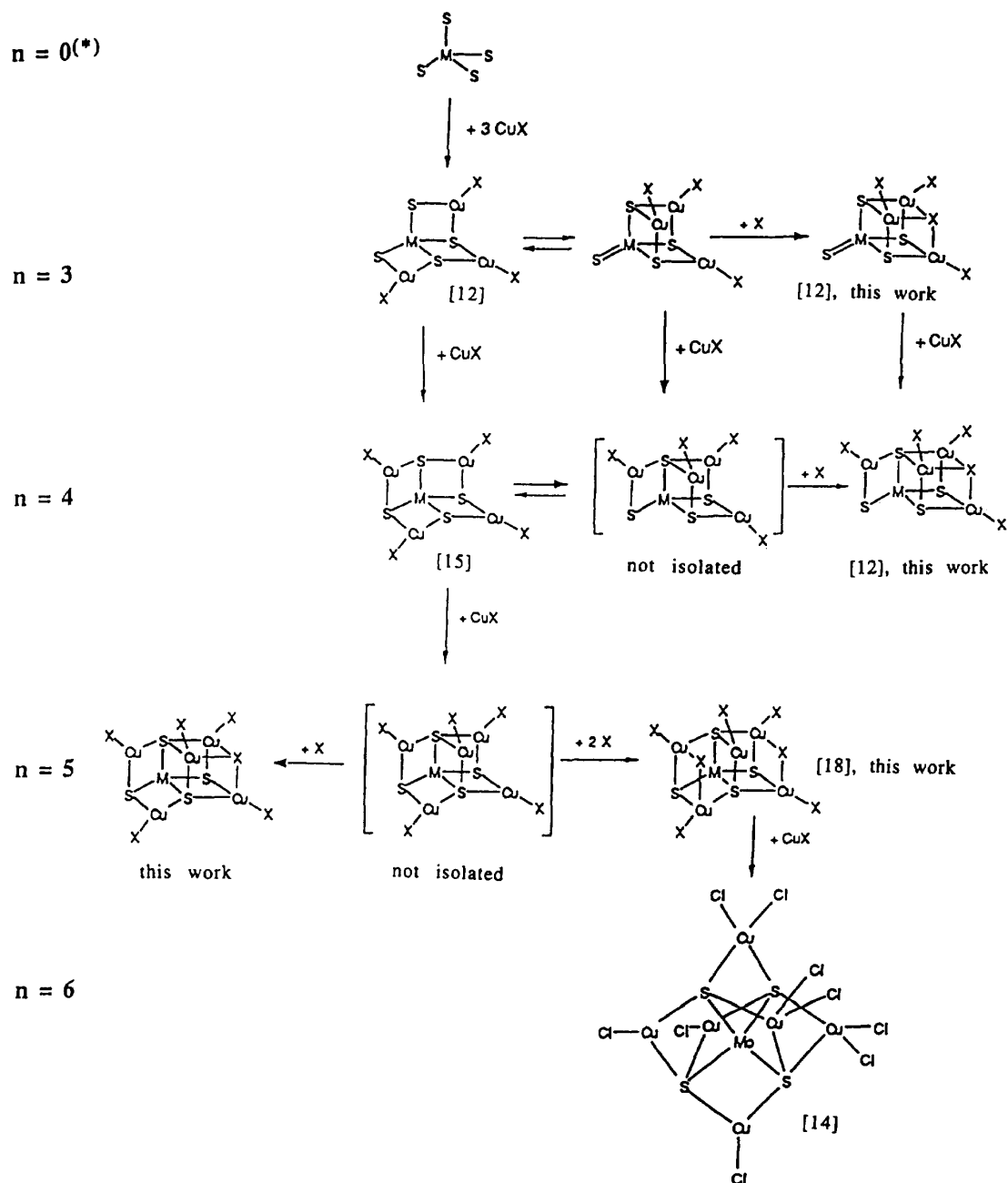
• $(\text{NPr}_4)_3[\text{WS}_4\text{Cu}_3\text{I}_4]$ **1**

To a solution of $(\text{NPr}_4)_2[\text{WS}_4]$ (0.340 g, 0.5 mmol) in 50 mL of dichloromethane were added under stirring CuI (0.286 g, 1.5 mmol) and $(\text{NPr}_4)\text{I}$ (0.500 g, 1.6 mmol). The resulting orange suspension turned red after 1 h of stirring at room temperature. The insoluble WS_4Cu_2 formed was filtered off and ether was added to the red filtrate. After several days at room temperature, 0.280 g of a red powder was recovered. Anal calc for $\text{C}_{36}\text{H}_{84}\text{N}_3\text{I}_4\text{S}_4\text{Cu}_3\text{W}$ **1**: C, 27.54; H, 5.36; N, 2.68; I, 32.38; S, 8.16; Cu, 12.14; W, 11.73. Found: C, 26.69; H, 5.15; N, 2.66; I, 32.35; S, 7.53; Cu, 12.48; W, 11.69.

• $(\text{NPr}_4)_3[\text{WS}_4\text{Cu}_3\text{Br}_4]$ **2**

The method used for **2** was similar to the preparation of **1** (yield, 72%). Compound **2** was identified by chemical analysis and spectroscopic measurements. Anal calc for $\text{C}_{36}\text{H}_{84}\text{N}_3\text{Br}_4\text{Cu}_3\text{W}$ **2**: C, 31.29; H, 6.08; N, 3.04; Br, 23.18;

* Correspondence and reprints



(*) n represents the number of Cu atoms coordinated to the central MS_4^{2-} ($\text{M} = \text{Mo}, \text{W}$).

Fig 1. Diagrammatic representation of the step-by-step addition of CuX ($\text{X} = \text{Cl}, \text{Br}, \text{I}$) to MS_4^{2-} ($\text{M} = \text{Mo}, \text{W}$).

S, 9.27; Cu, 13.80; W, 13.33. Found: C, 30.62; H, 5.89; N, 2.82; Br, 21.86; S, 8.68; Cu, 13.43; W, 12.61.

Compounds **1** and **2** display the cubane structure established by X-ray determination for the chlorinated homolog $[\text{WS}_4\text{Cu}_3\text{Cl}_4]^{3-}$ [12].

• $(\text{NPr}_4)_3[\text{WS}_4\text{Cu}_5\text{I}_6]$ **3**

To a suspension of **1** (0.528 g, 0.336 mmol), in 80 mL of dichloromethane was added under stirring a solution of CuCl

(0.017 g, 0.168 mmol) previously dissolved in 10 mL of degassed acetonitrile. A red solution was obtained within few minutes and maintained under stirring for 20 min. The volume of the solution was then reduced to ca 30 mL, and ether carefully layered. Within a few days at room temperature, 0.030 g of well-shaped red crystals was obtained. Anal calc for $\text{C}_{36}\text{H}_{84}\text{N}_3\text{I}_6\text{Cu}_5\text{W}$ **3**: C, 22.16; H, 4.31; N, 2.15; I, 39.09; S, 6.57; Cu, 16.29. Found: C, 23.68; H, 4.50; N, 2.45; I, 38.79; S, 6.68; Cu, 16.79.

• $(\text{NBu}_4)_3[\text{MoS}_4\text{Cu}_5\text{Cl}_6]$ **4**

To a solution of $(\text{NBu}_4)_2[\text{MoS}_4]$ (0.177 g, 0.25 mmol) in 30 mL of dichloromethane was added under stirring CuCl (0.15 g, 1.5 mmol). The resulting suspension was refluxed for 48 h, and then cooled to room temperature. After elimination of MoS_4Cu_2 as a black solid, ether was added to the filtrate leading to the crystallization at room temperature of $(\text{NBu}_4)_2[\text{MoS}_4\text{Cu}_4\text{Cl}_4]$ [15]. The filtrate was maintained for several days at -25°C to give 0.060 g of black crystals which were washed with ether. Anal calc for $\text{C}_{36}\text{H}_{108}\text{N}_3\text{Cl}_6\text{S}_4\text{Cu}_5\text{Mo}$ **4**: C, 38.91; H, 7.29; Cl, 14.39; S, 8.65; Cu, 21.45; Mo, 6.48. Found: C, 39.11; H, 7.33; Cl, 14.35; S, 7.91; Cu, 21.62; Mo, 6.70. The crystals were monoclinic, $a = 11.68(2)$, $b = 23.66(3)$, $c = 26.16(6)$ Å, $\beta = 94.4(2)^\circ$ but decomposed at room temperature within a few hours.

• $(\text{NBu}_4)_3[\text{WS}_4\text{Cu}_5\text{Cl}_6]$ **5**

The method used for **5** was similar to the preparation of **3**. Compound **5** was identified by spectroscopic measurements. Crystals of **5** also decomposed at room temperature within a few hours.

• $(\text{NEt}_4)_4[\text{WS}_4\text{Cu}_5\text{Cl}_7]$ **6**

To a solution of $(\text{NBu}_4)_2[\text{WS}_4\text{Cu}_4\text{Cl}_4]$ (0.240 g, 0.2 mmol) in 50 mL of acetonitrile was added under stirring NEt_4Cl (0.200 g, 1.2 mmol). After 20 min stirring, the solution was evaporated under reduced pressure to dryness. The red solid was recrystallized in acetonitrile (yield, 0.060 g, 20%). Anal calc for $\text{C}_{32}\text{H}_{80}\text{N}_4\text{Cl}_7\text{S}_4\text{Cu}_5\text{W}$ **6**: C, 27.47; H, 6.18; N, 4.00; Cl, 17.77; S, 9.16; Cu, 22.71; W, 13.16. Found: C, 27.63; H, 6.18; N, 4.05; Cl, 17.80; S, 8.48; Cu, 22.10; W, 13.17.

• $(\text{NEt}_4)_4[\text{WS}_4\text{Cu}_5\text{Br}_7]$ **7**

NEt_4Cl (0.066 g, 0.4 mmol) was added to a solution of $(\text{NPr}_4)_3[\text{WS}_4\text{Cu}_3\text{Br}_4]$ (0.276 g, 0.2 mmol) in 100 mL of dichloromethane. The orange-red solution was refluxed for 24 h and then cooled to room temperature. After the solution was reduced to 25 mL under reduced pressure, well-shaped red crystals were obtained within 24 h at room temperature (0.030 g). The chemical composition of **7** was deduced from the complete crystallographic study.

• $(\text{NEt}_4)_4[\text{WS}_4\text{Cu}_5\text{I}_{5.5}\text{Cl}_{1.5}]$ **8**

$(\text{NEt}_4)_2[\text{WS}_4]$ (0.170 g, 0.3 mmol) was suspended in 25 mL dichloromethane. To this suspension were added under stirring CuCl (0.088 g, 0.9 mmol) and NPr_4I (0.250 g, 0.8 mmol). After 30 min of stirring at room temperature the red precipitate formed was eliminated and 5 mL ether added to the filtrate. Red crystals suitable for X-ray analysis were obtained within several days (0.015 g).

• $(\text{NMe}_4)_4[\text{WS}_4\text{Cu}_5\text{Cl}_7]$ **9**

$(\text{NBu}_4)_2[\text{WS}_4\text{Cu}_4\text{Cl}_4]$ (0.100 g, 0.084 mmol) was dissolved in 100 mL of acetonitrile. After addition of NMe_4Cl (0.036 g, 0.336 mmol) and CuCl (0.0085 g, 0.084 mmol), the solution was stirred for 1 h at room temperature. A black precipitate was obtained by reduction of the volume of the solution to 25 mL, and spectroscopically identified by comparison with compound **7**.

• $(\text{NMe}_4)_4[\text{MoS}_4\text{Cu}_5\text{Cl}_7]$ **10**

This was obtained *via* a similar route as **9** starting from $(\text{NBu}_4)_2[\text{MoS}_4\text{Cu}_4\text{Cl}_4]$.

• $(\text{NMe}_4)_5[\text{MoS}_4\text{Cu}_6\text{Cl}_9]$ **11**

a) To a solution of **10** (0.040 g, 0.036 mmol) in 40 mL of acetonitrile was added 3.6 mL of a solution of CuCl 10^{-2}M (0.036 mmol) in degassed acetonitrile. After stirring

for about 1 h at room temperature the solution was reduced to 10 mL. The black precipitate formed was recrystallized in acetonitrile and black needles with hexagonal sections suitable for X-ray analysis were obtained.

b) This compound was also obtained by addition of CuCl (0.020 g, 0.2 mmol) and NMe_4Cl (0.055 g, 0.5 mmol) on $(\text{NBu}_4)_2[\text{MoS}_4\text{Cu}_4\text{Cl}_4]$ (0.110 g, 0.1 mmol) previously dissolved in 100 mL degassed acetonitrile. After 1 h of stirring, the violet solution was reduced to 50 mL prior to standing few days at room temperature. The black crystals formed were identified by X-ray determination. The crystals were orthorhombic, space group $\text{Cmc}2_1$, $a = 19.945(3)$, $b = 11.513(1)$, $c = 20.541(7)$ Å. The complete resolution of the structure was reported in a previous publication [14].

• $(\text{NMe}_4)_5[\text{WS}_4\text{Cu}_6\text{Cl}_9]$ **12**

Addition of CuCl to **9** led to a red powder, identified by comparison with **11** by IR and UV-vis spectroscopies, and chemical analysis. Anal calc for $\text{C}_{20}\text{H}_{60}\text{N}_5\text{Cl}_9\text{S}_4\text{Cu}_6\text{W}$ **12**: C, 17.33; H, 5.78; N, 5.05. Found: C, 17.98; H, 4.32; N, 4.98.

Crystal structure determinations

Unit cell dimensions for compounds **3**, **6**, **7** and **8** were obtained from least-squares refinement of the setting angles of 25 reflections. Intensity data were collected at room temperature with a $\theta - 2\theta$ scan technique on a Enraf-Nonius CAD4 four-circle diffractometer. Two standard reflexions were monitored periodically; they showed no change during data collection. Crystallographic data and pertinent information are given in table I. Corrections for polarization and Lorentz effects were applied. Absorption was corrected by Difabs [15]. Computations were performed using the Crystals programme [16] adapted for a Micro Vax II. Atomic form factors for neutral W, Cu, C, N, S, Cl, Br and I were taken from reference [17]. The structure was solved by interpretation of Patterson maps, followed by the use of successive difference Fourier maps. Hydrogen contributions were omitted. Least-squares refinements with approximation to the normal matrix were carried out by minimizing the function $\Sigma \omega(|F_o| - |F_c|)^2$, where F_o and F_c are the observed and calculated structure factors. The weighting scheme used is $\omega = \omega' / [1 - (\Delta F / 6\sigma(F))^2]$ with $\omega' = 1 / \Sigma_n^2 \text{ArTr}(X)$ where n ($n = 3$) is the number of coefficients, Ar, for a Chebyshev series, for which X is F_c / F_o (max). The model reached convergence with $R = \Sigma(|F_o| - |F_c|) / \Sigma|F_o|$ and $R_w = [\Sigma \omega(|F_o| - |F_c|)^2 / \Sigma \omega(F_o)^2]^{1/2}$ values listed in table I. Criteria for a satisfactory complete analysis were the ratios of the rms shift to standard deviation at less than 0.1 and no significant features in final difference map.

Results and discussion

Crystal structure determinations

All structures consist of well-separated cations and anions. In all structures, cations have normal bond distances and angles (see *Supplementary material*).

• *Structure of $(\text{NPr}_4)_3[\text{WS}_4\text{Cu}_5\text{I}_6]$ **3***

The space group Pbnm (standard group Pnma No 62) was chosen from the evidence of the two systematic extinctions $0kl$, $k = 2n + 1$, and $h0l$, $h + l = 2n + 1$, and the results of statistical tests of centrosymmetry. Positional atomic coordinates are given in table II, and selected geometrical parameters in table III. A view of the $[\text{WS}_4\text{Cu}_5\text{I}_6]^{3-}$ anion is given in figure 2, including

Table I. Crystal data and data collection for the structures of (NPr₄)₃[WS₄Cu₅I₆] **3**, (NEt₄)₄[WS₄Cu₅Cl₇] **6**, (NEt₄)₄[WS₄Cu₅Br₇] **7** and (NEt₄)₃[WS₄Cu₅Cl_{1.5}I_{5.5}] **8**.

Formula	C ₃₆ H ₈₄ N ₃ I ₆ S ₄ Cu ₅ W 3	C ₃₂ H ₈₀ N ₄ Cl ₇ S ₄ Cu ₅ W 6	C ₃₂ H ₈₀ N ₄ Br ₇ S ₄ Cu ₅ W 7	C ₃₂ H ₈₀ N ₄ Cl _{1.5} I _{5.5} S ₄ Cu ₅ W 8
M	1 949.5	1 399.0	1 710.1	1 902.0
Crystal system	orthorhombic	monoclinic	monoclinic	monoclinic
Space group	<i>Pbnm</i>	<i>C2/c</i>	<i>C2/c</i>	<i>C2/c</i>
<i>a</i> /Å	13.130(6)	22.626(9)	22.866(5)	23.246(3)
<i>b</i> /Å	20.829(12)	10.672(6)	10.769(2)	10.762(2)
<i>c</i> /Å	22.715(5)	21.613(9)	21.960(9)	22.374(4)
α /°	90	90	90	90
β /°	90	94.17(4)	94.23(3)	93.62(1)
γ /°	90	90	90	90
<i>U</i> /Å ³	6 212(5)	5 205(15)	5 364(12)	5 586
<i>Z</i>	4	4	4	4
Dc/gcm ⁻³	2.08	1.78	2.12	2.26
<i>F</i> (000)	3 688	2 808	3 312	3 600
μ /cm ⁻¹	66.8		94.8	72.2
θ limits/°	1–23		1–20	1–25
Reflections collected	4 821		2 822	5 335
used	1 696		1 453	3 055
<i>R</i>	0.0504		0.0626	0.0688
<i>R'</i>	0.0606		0.0733	0.0826
Refined parameters	269		243	252

Details in common: Enraf-Nonius diffractometer ($\lambda = 0.71069$ Å), $\theta - 2\theta$ scan type, scan range $0.8 + 0.345 \tan \theta$, $R = (|F_o - F_c|)/|F_o|$, $R' = (\omega(|F_o| - |F_c|)^2 / \omega F_o^2)^{1/2}$.

the labelling scheme. The W(1), S(2), and S(3) atoms are located in the mirror plane, and the geometry of the WS₄ tetrahedron is achieved by the S(1) out of plane atom. The Cu(3)-I(3) group lies in the mirror, the Cu(1)-I(1) and Cu(2)-I(2) groups being in general position which generates a cluster with five copper atoms. The geometry of the cluster is completed by the μ^3 -I(4) atom bridging the Cu(2), Cu(3) and Cu(2)' atoms.

Despite the apparent dissymmetry of the anion (*C_s* point group), the central WS₄ core has retained the parent tetrahedral geometry with a mean S-W-S angle of 109.5(6)°. The five copper atoms are bonded to the WS₄

tetrahedron through sulfur double bridges, and display two types of environment: (i) the two equivalent Cu(1) and Cu(1)' atoms have a distorted trigonal environment with angles in the range 107.3(3)–127.6(3)°, and the W(1)S(1)S(2)Cu(1)'I(1)' and W(1)S(1)'S(2)Cu(1)I(1) fragments are planar (mean deviation for W = 0.105 Å); or (ii) Cu(2), Cu(2)', and Cu(3) are tetracoordinated, which results in the lengthening of the Cu-S bond, 2.263 (4) Å in comparison with the 2.34 (4) Å observed for the trigonal Cu(1) atom (such a correlation between the coordination of a copper atom and the corresponding Cu-S bond length has already been observed for the [WS₄Cu₄Cl₅]³⁻ cubane [18]).

Each copper atom is also bonded to a terminal iodide, the Cu-I distances having expected values in the range 2.404(4)–2.459(4) Å. The coordination at the Cu(2), Cu(2)' and Cu(3) atoms is achieved by the triply bridging I(4) atom. Such an unusual coordination for iodine results in the lengthening of the bonds attached to this atom; the Cu-I(4) distances are in the range 2.827(5)–2.940(4) Å. These values can be considered as bonding distances since they are weaker than the sum of the ionic radii of Cu(+) and I(-), *ie* 2.99 Å. The bridging character of I(4) is also confirmed by the low value of the thermal parameter observed for this atom, *U* = 0.06, compared to the related mean value *U* = 0.09 for the terminal I(1), I(2), and I(3) atoms.

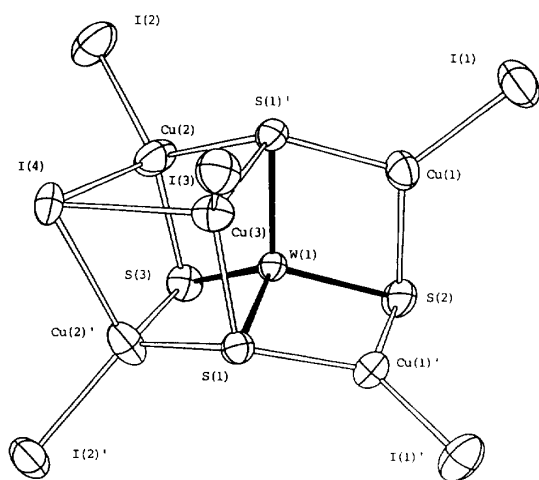
The five copper atoms form a rectangular pyramid with the W atom located 0.27 Å below the

Table II. Atom coordinates and isotropic displacement parameters for compound **3**.

Atom	<i>x/a</i>	<i>y/b</i>	<i>z/c</i>	<i>U</i> (equ)
W(1)	0.2089(1)	0.09770(6)	0.2500	0.0404
S(1)	0.1767(4)	0.1567(3)	0.1694(2)	0.0506
S(2)	0.1049(8)	0.0123(4)	0.2500	0.0610
S(3)	0.3694(7)	0.0655(4)	0.2500	0.0584
Cu(1)	0.0594(2)	0.0776(1)	0.1746(1)	0.0626
Cu(2)	0.3562(2)	0.1451(2)	0.3204(1)	0.0738
Cu(3)	0.1691(4)	0.2256(2)	0.2500	0.0644
I(1)	-0.0819(2)	0.0649(1)	0.1083(1)	0.0954
I(2)	0.4685(2)	0.1504(1)	0.40690(9)	0.0856
I(3)	0.0662(2)	0.3225(2)	0.2500	0.0914
I(4)	0.3761(2)	0.2630(1)	0.2500	0.0609

Table III. Bond lengths (Å) and angles (deg) for compound **3**.

W(1)-S(1)	2.244(6)	W(1)-S(3)	2.211(9)
W(1)-S(2)	2.242(9)		
W(1)···Cu(1)	2.639(3)	Cu(2)···Cu(2)	3.197(7)
W(1)···Cu(2)	2.697(3)	Cu(2)···Cu(3)	3.376(5)
W(1)···Cu(3)	2.715(4)		
S(1)-W(1)-S(1)	109.2(3)	S(2)-W(1)-S(1)	108.6(2)
S(3)-W(1)-S(1)	110.2(2)	S(3)-W(1)-S(2)	109.9(3)
S(1)-Cu(1)	2.259(6)	S(2)-Cu(1)	2.267(7)
S(1)-Cu(2)	2.380(7)	S(3)-Cu(2)	2.311(7)
S(1)-Cu(3)	2.328(6)		
Cu(1)-S(1)-W(1)	71.7(2)	Cu(2)-S(1)-Cu(1)	126.6(3)
Cu(2)-S(1)-W(1)	71.3(2)	Cu(3)-S(1)-Cu(1)	112.3(3)
Cu(3)-S(1)-W(1)	72.8(2)	Cu(3)-S(1)-Cu(2)	91.6(2)
Cu(1)-S(2)-W(1)	71.6(2)	Cu(1)-S(2)-Cu(1)	98.2(4)
Cu(2)-S(3)-W(1)	73.2(2)	Cu(2)-S(3)-Cu(2)	87.5(3)
Cu(1)-I(1)	2.404(4)		
Cu(2)-I(2)	2.459(4)	Cu(2)-I(4)	2.940(4)
Cu(3)-I(3)	2.429(5)	Cu(3)-I(4)	2.827(5)
S(2)-Cu(1)-S(1)	107.3(3)	I(1)-Cu(1)-S(2)	127.6(3)
I(1)-Cu(1)-S(1)	125.1(2)		
S(3)-Cu(2)-S(1)	102.3(3)	I(2)-Cu(2)-S(1)	120.7(2)
I(2)-Cu(2)-S(3)	122.7(2)	I(4)-Cu(2)-S(1)	93.2(2)
I(4)-Cu(2)-S(3)	102.5(2)	I(4)-Cu(2)-I(2)	110.1(1)
S(1)-Cu(3)-S(1)	103.7(3)	I(3)-Cu(3)-S(1)	122.4(2)
I(4)-Cu(3)-S(1)	97.4(2)	I(4)-Cu(3)-I(3)	107.8(2)
Cu(2)-I(4)-Cu(2)	65.9(1)	Cu(3)-I(4)-Cu(2)	71.6(1)

**Fig 2.** Ortep representation of compound **3**. Half of the anion (primed atoms) is generated through the mirror plane passing through S(3), I(4), Cu(3) and S(2).

Cu(1)Cu(1')Cu(2)Cu(2') basal plane. The [W(1)S(1)S(1')S(3)Cu(2)Cu(2')Cu(3)I(4)] fragment displays a distorted cubic geometry with angles ranging from 62.9(1)° to 110.2(2)°, far from the ideal value of 90°, and edges in the wide range 2.211(9)–2.940(4) Å. Calculations of the mean planes formed by the six faces of the cube show that the atoms which most participate in the deformation are those pertaining to the central WS₄ group as shown in table IV. These observations,

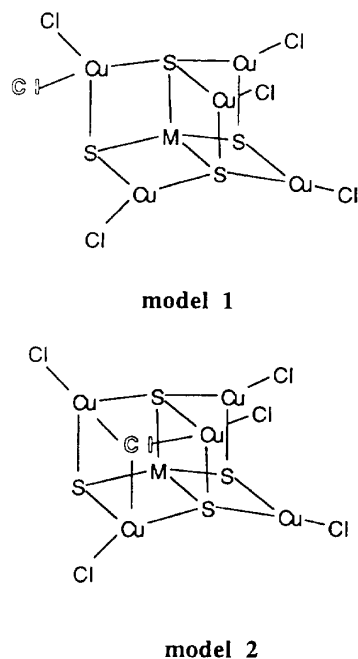
together with the evidence of ideal geometric parameters for WS₄, caused us to consider this fragment as a rigid group.

Table IV. Mean-plane deviations (Å) in compound **3**.

Mean plane	Deviation	Atom
W(1)S(1)Cu(3)S(1)'	0.094	W(1)
W(1)S(1)S(3)Cu(2)'	0.136	W(1)
W(1)S(1')S(3)Cu(2)	0.136	W(1)
I(4)Cu(3)S(1')Cu(2)	0.243	S(1)'
I(4)Cu(3)S(1)Cu(2)'	0.243	S(1)
I(4)Cu(2)S(3)Cu(2)'	0.122	S(3)

[MS₄Cu₅Cl₆]³⁻ homologs (M = Mo **4** and M = W **5**) have the same chemical composition and similar IR spectra as **3**. This means that although no structural determination is available because of the poor stability of the crystals, it can be assumed that **4** and **5** have the same overall geometry as **3**.

The addition of five CuCl groups to the S-S edges of the MS₄ tetrahedron so that a free edge remained uncoordinated led to a single possibility for the structure of the resulting MS₄Cu₅ fragment, because the six S-S edges in a tetrahedron are equivalent. In contrast, two possibilities exist for the addition of a sixth halide to the former MS₄Cu₅ core, as represented in figure 3.

**Fig 3.** Possible geometries for the [MS₄Cu₅Cl₆]³⁻ anion.

In model 1, the sixth halide is located in the terminal position and bonded to one of the five equivalent copper atoms of the [WS₄(CuCl)₅] moiety. The final compound has thus retained the open structure of the [WS₄Cu₅] parent core. In model 2, the additional halide forms a

μ^3 -Cl bridge leading to the cubane structure observed for **3**, **4** and **5**. Only isomers corresponding to model 2 were isolated.

- Structures of $(NEt_4)_4[WS_4Cu_5X_7]$, $X = Cl$ **6**, $X = Br$ **7**, $X = Cl$ and **8**

Pertinent crystallographic data are listed in table I, and bond distances for **7** are given in table V. The three compounds are isostructural, with an expected increase of the volume cell by replacing chlorine by bromine and iodine. A statistical disorder is observed for **8**; the bridging site between Cu(1) and Cu(2) is occupied by the two atoms, I(4) and Cl(4). Refinement of the occupancy factor of this site converged to 0.25 for I(4) and 0.75 for Cl(4), leading to the anionic composition $[WS_4(CuI)_5I_{0.5}Cl_{1.5}]^{4-}$.

Table V. Bond lengths (Å) and angles (degrees) for compound **7**.

W(1)-S(1)	2.271(6)	W(1)-S(2)	2.207(7)
W(1)···Cu(1)	2.698(3)	Cu(1)···Cu(2)	3.214(5)
W(1)···Cu(2)	2.689(3)		
W(1)···Cu(3)	2.673(5)		
S(1)-W(1)-S(1)	108.3(3)	S(2)-W(1)-S(1)	110.0(2)
S(2)-W(1)-S(1)	109.9(2)	S(2)-W(1)-S(2)	108.7(4)
S(1)-Cu(1)	2.372(7)	S(1)-Cu(2)	2.357(7)
S(2)-Cu(1)	2.314(7)	S(2)-Cu(2)	2.310(7)
S(1)-Cu(3)	2.279(7)		
Cu(1)-S(1)-W(1)	71.0(2)	Cu(2)-S(1)-Cu(1)	129.1(3)
Cu(2)-S(1)-W(1)	71.0(2)	Cu(3)-S(1)-Cu(1)	99.0(3)
Cu(3)-S(1)-W(1)	71.9(2)	Cu(3)-S(1)-Cu(2)	100.2(3)
Cu(1)-S(2)-W(1)	73.2(2)	Cu(2)-S(2)-Cu(1)	88.1(2)
Cu(2)-S(2)-W(1)	73.0(2)		
Cu(1)-Br(1)	2.299(4)	Cu(2)-Br(2)	2.272(5)
Cu(1)-Br(4)	2.644(5)	Cu(2)-Br(4)	2.675(5)
Cu(3)-Br(3)	2.269(6)		
S(2)-Cu(1)-S(1)	102.9(3)	S(2)-Cu(2)-S(1)	103.7(3)
Br(1)-Cu(1)-S(1)	121.5(2)	Br(2)-Cu(2)-S(1)	121.1(2)
Br(1)-Cu(1)-S(2)	123.1(2)	Br(2)-Cu(2)-S(2)	122.4(3)
Br(4)-Cu(1)-S(1)	99.1(2)	Br(4)-Cu(2)-S(1)	97.9(2)
Br(4)-Cu(1)-S(2)	97.3(2)	Br(4)-Cu(2)-S(2)	96.5(2)
Br(4)-Cu(1)-Br(1)	107.7(2)	Br(4)-Cu(2)-Br(2)	109.9(2)
S(1)-Cu(3)-S(1)	107.8(3)	Br(3)-Cu(3)-S(1)	126.1(2)
Cu(2)-Br(4)-Cu(1)	74.3(1)		

The geometry of **8** represented in figure 4 is similar to the previously reported structure for $[WS_4Cu_5Cl_7]^{4-}$ [18], consisting of a cage of 12 atoms with a binary axis passing through W, Cu(3) and X(3) ($X = Br$ for **7**, $X = I$ for **8**). This geometry results from the addition of five copper atoms across five S-S edges of the WS_4 tetrahedron leaving the remaining edge uncoordinated. The four copper atoms Cu(1)Cu(1')Cu(2)Cu(2)' form the basal plane of a rectangular pyramid with the tungsten atom located below the basal plane, 0.34 Å for **7** and 0.38 Å for **8**. A terminal halide is attached to each copper atom through normal bond lengths, 2.28(2) Å for **7** and 2.43(2) Å for **8**. The geometry is completed by the bridging Br(4) atom for **7**, and a mixture of 0.75 Cl(4) and 0.25 I(4) for **8**.

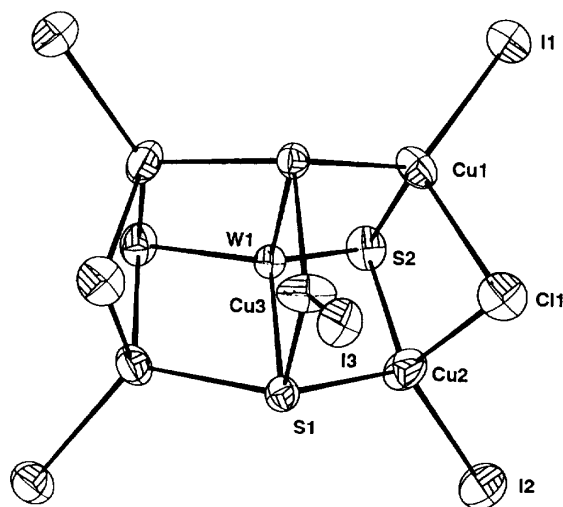


Fig 4. Ortep drawing of compound **8**. $X = 0.25 I + 0.75 Cl$.

- Structure of $[MS_4Cu_6Cl_9]^{5-}$ **11** and **12**

The molecular arrangement of **11** and **12** is given in figure 5. The complete X-ray structure was recently published in a preliminary report [14]. The anionic cluster is formed of a central MS_4 tetrahedron encapsulated in a distorted octahedron of copper atoms; the local symmetry is lowered to C_{3v} . Three copper atoms have a trigonal environment while the three others are tetra coordinated. The central MoS_4 core retains the ideal geometry of the MoS_4 precursor confirming that this rigid group acts as a strong assembling core.

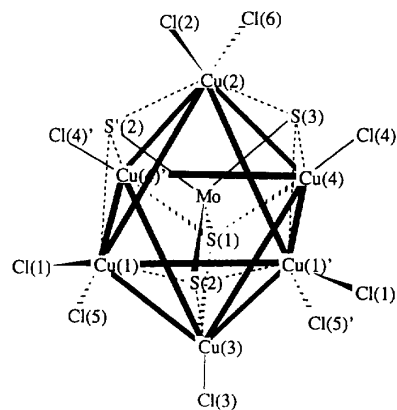


Fig 5. Representation of the molecular structure of **11** showing the MS_4 tetrahedron in an octahedral cage of copper atoms.

Syntheses

- Addition to the cubane structure $[MS_4Cu_3X_4]^{2-}$

In the cubane series $[MS_4Cu_3X_4]^{2-}$ ($M = Mo, W$, and $X = Cl, Br, I$) the μ^3 -bridging halide is labile allowing the solution transformation of a closed cubane structure into an open structure. This type of equilibrium

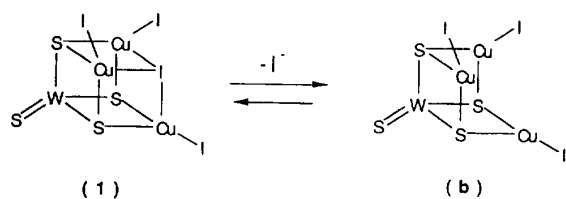


Fig 6. Representation of the equilibrium between cubane and pseudo-cubane structures.

between cubane and pseudo-cubane has been reported previously [12], and is represented in figure 6.

Two CuCl groups can be added across two free edges of the fully iodinated pseudo-cubane (b) to give the reactive transient species (i) whose structure could correspond to that described above for model 1. Fixation of a bridging iodide together with substitution of terminal chloro ligands by iodides led to compound **3**. CuCl was used in this synthesis in the place of CuI to illustrate the lability of chloro-ligands relative to iodides; the softer ligand I^- remains bonded to the soft metal Cu^+ . The corresponding reaction scheme is given in figure 7.

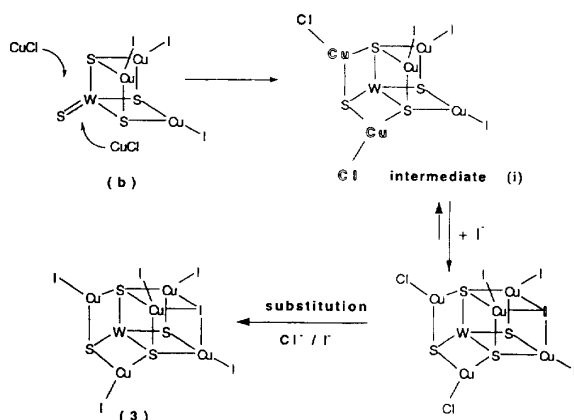


Fig 7. Diagrammatic representation of the synthesis of **3** from the cubane precursor $[MS_4Cu_3I_4]^{3-}$.

• Addition to the open-structure $[MS_4Cu_4X_4]^{2-}$

The reactive intermediate species $[MS_4Cu_5Cl_5]^{2-}$ (i) resulted from direct addition of CuCl to $[MS_4Cu_4Cl_4]^{2-}$. Addition to (i) of a chloride in a μ^3 -position led to compound **4**, which in the presence of additional chlorides at room temperature led to the final dicubane structure **6**. This sequence was performed by addition of two equivalents of NEt_4Cl together with CuCl to the starting $[WS_4Cu_4Cl_4]^{2-}$.

• Addition to the dicubane structure $[MS_4(CuCl)_5Cl_2]^{4-}$

One equivalent of CuCl was added to the dicubane structure **10** resulting in the formation of the copper-rich cluster **11**. This addition required first the cleavage of two μ^2 -Cl bridges of the dicubane structure and

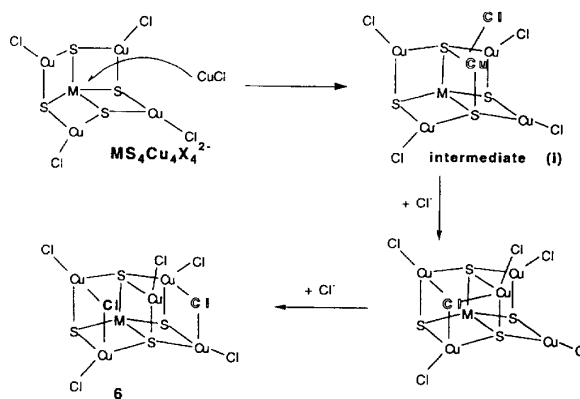


Fig 8. Diagrammatic representation of the formation of **6** from the open precursor $[MS_4Cu_4X_4]^{2-}$.

the addition of a supplementary chloride in terminal position as represented in figure 9.

The same final compound **11** was also obtained by addition of two equivalents of CuCl to $[MoS_4Cu_4Cl_4]^{2-}$, a precursor with an open structure, in the presence of additional NMe_4Cl . This reaction was clearly dependent on the stoichiometry in CuCl confirming that the fixation of CuCl on $[MS_4Cu_4Cl_4]^{2-}$ proceeded through the two following steps:

- (1) $[MS_4Cu_4Cl_4]^{2-} + CuCl + 2 Cl^- \rightarrow [MS_4Cu_5Cl_7]^{4-}$ evidenced by the formation of **9** and **10**
- (2) $[MS_4Cu_5Cl_7]^{4-} + CuCl + Cl^- \rightarrow [MS_4Cu_6Cl_9]^{5-}$ illustrated by the formation of **11**

$[MoS_4Cu_6Cl_9]^{5-}$ **11**, was also obtained as crystals by direct addition of CuCl on $[MoS_4]^{2-}$ [14].

Discussion on copper-rich structures

In the various structures described above, each copper atom is bonded to terminal and bridging halides. A relationship exists between the number of halo-bridges present in a polythiometalate and its architecture. The more closed the structure, the less halo-bridges it contains. In $[MS_4Cu_5I_6]^{3-}$ **3**, **4** and **6**, and $[MS_4Cu_5X_7]^{4-}$ **6-9**, one μ^3 -X (X = Cl, Br, I) and two μ^2 -X bridges are observed, respectively, while no bridging halide is present in the closest cluster $[MS_4Cu_6Cl_9]^{5-}$ **11**. Copper atoms in complexes with the Cu_5M composition form a Cu_5 cage described as a rectangular pyramid. To these five copper atoms are attached different halides (X = Cl, Br, I) in variable stoichiometries (**6** and **7**), both in bridging and terminal positions. In table VI, we give geometric data for these compounds.

As expected, $Cu-X_{term}$ bond lengths increase along with the atomic number of the terminal halide, but in contrast, distances between copper and bridging halides, namely $Cu-X_{brid}$, are more or less independent of the nature of the halogen. Moreover, μ^3 -X bridges are probably engaged in weaker bonds than μ^2 -X bridges if the bond length reflects the bond strength. The non-bonding $Cu(3)$ -X distances in **3**, **7** and **8** increase while

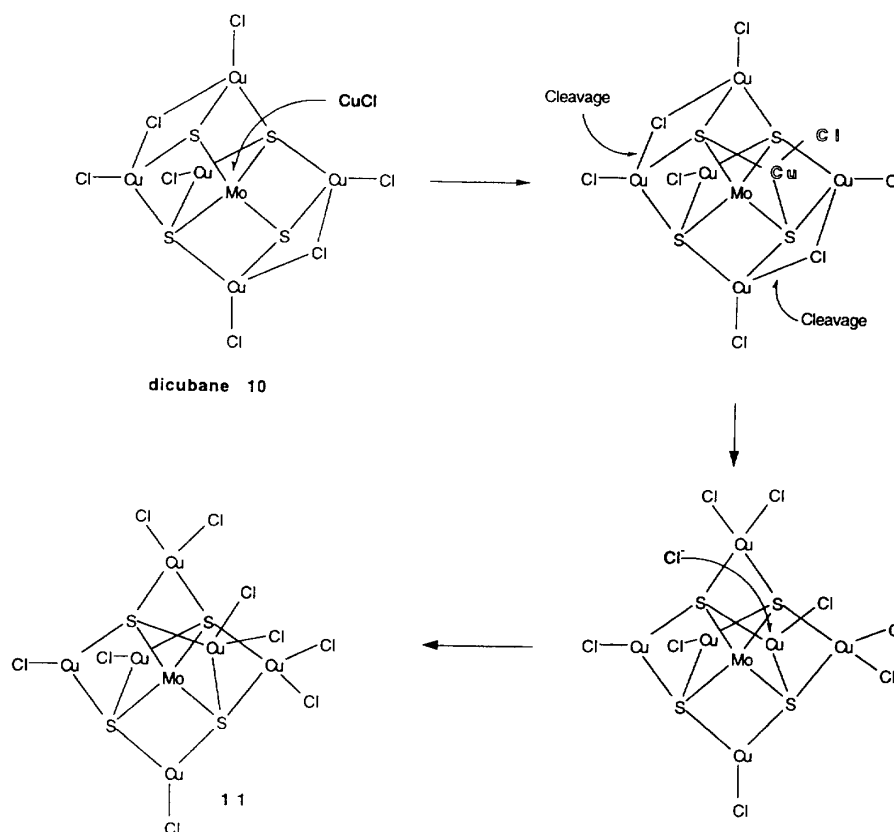


Fig 9. Representation of the formation of **11** from the dicubane precursor $[\text{MS}_4\text{Cu}_5\text{Cl}_7]^{4-}$

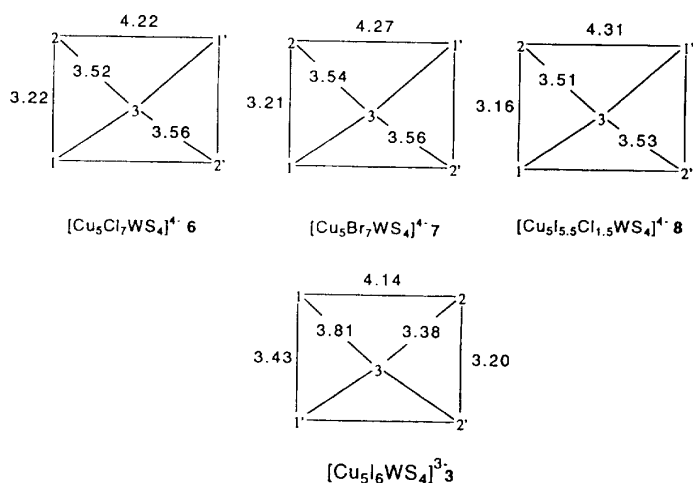


Fig 10. Projection of the Cu_5 pyramid in the basal plane showing the geometric dimensions in $[\text{WS}_4\text{Cu}_5\text{X}_7]^{4-}$ X = Cl, Br, I.

chloride is replaced by a heavier halide, which provokes the distortion of the Cu_5 pyramid as represented in figure 10.

In the basal plane of the Cu_5 pyramid the $\text{Cu}(1)\text{-Cu}(2')$ and $\text{Cu}(2)\text{-Cu}(1')$ distances increase significantly while the other two decrease. The other edges of the pyramid vary shortly in the range 3.51–3.56 Å so that

the basal area of the pyramid remains nearly constant in the range 13.61–13.72 Å². Calculations of the inter-halide distances in the different structures show that the distortion can be considered as an adaptation of the Cu_5 cluster which minimizes the interactions between the terminal atoms attached to the four copper atoms of the basal plane. In $[\text{WS}_4\text{Cu}_5\text{I}_6]^{3-}$ **3**, the four copper

Table VI. Cu-X bond lengths (Å) for cubane structures **3** and **6–8**.

Compound		Cu-X _{term}	Cu-X _{brid}	Cu(3)-X
(NMe ₄) ₄ [WS ₄ (CuCl) ₅ Cl ₂]	6 ^a	2.18(2)	2.63(12)	3.188(2)
(NEt ₄) ₄ [WS ₄ (CuBr) ₅ Br ₂]	7	2.28(1)	2.66(2)	3.274(2)
(NEt ₄) ₄ [WS ₄ (CuI) ₅ X ₂]	8	2.43(2)	2.67(4)	3.274(4)
(NPr ₄) ₃ [WS ₄ Cu ₅ I ₆]	3	2.43(3)	2.90(6)	

^a From ref [18]. For **3**, X = 0.25I + 0.75Cl.

atoms forming the basal plane are not equivalent which leads to an additional deformation of the cluster; Cu(2) and Cu(2') are bonded to a bridging iodide while Cu(1) and Cu(1') are not engaged in any bridge. Thus, the symmetry of the Cu₅ cluster is lowered from *C*_{2v} (**7**, **8**) to *C*_s (**3**), resulting in the dimensions given in figure 10.

Supplementary material available

Complete X-ray data for compounds **3** and **6–8**, including tables of interatomic distances, thermal parameters (tables S1 to S4), calculated and observed structure factors (17 pages in reduced form) are available from the British Library, Document Supply Centre at Boston Spa, Wetherby, West Yorkshire, UK, as supplementary publication N° SUP 90392.

References

- 1 Holm RH, *Chem Soc Rev* (1981) 10, 55
- 2 Coucouvanis D, *Acc Chem Rev* (1981) 14, 201
- 3 Müller A, Diemann E, Jostes R, Bögge H, *Angew Chem, Int Ed Engl* (1981) 20, 934
- 4 Müller A, Jaegermann W, Enemark JH, *Coord Chem Rev* (1982) 46, 245
- 5 Averill BA, *Struct Bond, Berlin* (1983) 53, 59
- 6 Draganjac M, Rauchfuss TB, *Angew Chem, Int Ed Engl* (1985) 24, 742
- 7 Müller A, *Polyhedron* (1986) 5, 323
- 8 Coucouvanis D, Hadjikyriacou A, Draganjac M, Kanatzidis MG, Ileperuma O, *Polyhedron* (1986) 5, 349
- 9 Müller A, Diemann E, *Adv Inorg Chem Radiochem* (1987) 31, 89
- 10 DuBois MR, *Chem Rev* (1989) 89, 1
- 11 Eldredge PA, Averill BA, *J Cluster Sci* (1990) 1, 269
- 12 a) Jeannin Y, Sécheresse F, Bernès S, Robert F, *Inorg Chim Acta* (1992) 198-200, 493
b) Müller A, Krickemeyer E, Hildebrand A, Bögge H, Schneider K, Lemke M, *J Chem Soc, Chem Commun* (1991) 1685
- 13 Sécheresse F, Bernès S, Robert F, Jeannin Y, *J Chem Soc Dalton Trans* (1991) 2875
- 14 Bernès S, Sécheresse F, Jeannin Y, *Inorg Chim Acta* (1992) 191, 11
- 15 Walker N, Stuart D, *Acta Crystallogr, Sect A* (1983) 39, 158
- 16 Watkin DJ, Carruthers JK, Betteridge PW, Crystals, an advanced crystallographic program system, Chemical Crystallography Laboratory, University of Oxford, 1988
- 17 International Tables for X-Ray Crystallography, Kynoch Press, Birmingham, vol 4 (1974)
- 18 Sécheresse F, Manoli JM, Potvin C, Marzak S, *J Chem Soc Dalton Trans* (1988) 3055